Lawrence Berkeley National Laboratory

Lawrence Berkeley National Laboratory

Title

Lithographic measurement of EUV flare in the 0.3-NA Micro Exposure Tool optic at the Advanced Light Source

Permalink

https://escholarship.org/uc/item/3800c1p5

Authors

Cain, Jason P.
Naulleau, Patrick
Spanos, Costas J.

Publication Date

2005

eScholarship.org Powered by the California Digital Library
University of California

Lithographic measurement of EUV flare in the 0.3-NA Micro Exposure Tool optic at the Advanced Light Source

Jason P. Cain,[a1] Patrick Naulleau,[b] Costas J. Spanos[a]

[a] Department of Electrical Engineering and Computer Sciences,
University of California, Berkeley, CA 94720
[b] Center for X-Ray Optics, Lawrence Berkeley National Laboratory, Berkeley, CA 94720

ABSTRACT

The level of flare present in a 0.3-NA EUV optic (the MET optic) at the Advanced Light Source at Lawrence Berkeley National Laboratory is measured using a lithographic method. Photoresist behavior at high exposure doses makes analysis difficult. Flare measurement analysis under scanning electron microscopy (SEM) and optical microscopy is compared, and optical microscopy is found to be a more reliable technique. In addition, the measured results are compared with predictions based on surface roughness measurement of the MET optical elements. When the fields in the exposure matrix are spaced far enough apart to avoid influence from surrounding fields and the data is corrected for imperfect mask contrast and aerial image proximity effects, the results match predicted values quite well. The amount of flare present in this optic ranges from 4.7% for 2 µm features to 6.8% for 500 nm features.

Keywords: Extreme ultraviolet (EUV) lithography, flare, micro-exposure tool (MET) optic, synchrotron

1. INTRODUCTION

Roughness (also known as finish errors) on the optical surfaces of higher spatial frequency than aberrations leads to non-specular scattering of light. The high-spatial frequency roughness will scatter light out of the image, reducing the throughput, while the mid-spatial frequency roughness (spatial frequencies in the 1/mm to 1/µm range[1] will scatter light within the field of view. This phenomenon is known as flare (also called stray light), and in general it leads to a reduced aerial image contrast and therefore a reduced process window. The amount of flare present in an optical system is most often expressed as a percentage of the light in the clear field that appears in the dark areas. While the flare for DUV lithography tools has been reported to be about 2-6%[2,3] the flare in early EUV lithography tools has been shown to be as high as 20-40%[4]. Production EUV lithography tools will need to achieve a flare level of less than 10% in order to meet CD control requirements[5].

The total integrated scatter (TIS) is defined as the ratio of the non-specular scattered power to the reflected specular power when light is incident on a surface. The TIS is given by[6]

$$\text{TIS} = \frac{P_s}{RP_i} = \frac{P_s}{P_0} \cong \left(\frac{4\pi\sigma_s \cos\theta_i}{\lambda} \right)^2 , \tag{1}$$

where P_s is scattered power, R is the reflection coefficient, P_i is incident power, P_0 is specular reflected power, σ_s is the standard deviation of the surface roughness, θ_i is the angle of incidence, and λ is the wavelength of light illuminating the surface. As Equation 1 shows, TIS is proportional to $1/\lambda^2$. Therefore, as the wavelength of illumination is decreased in an effort to increase resolution, the flare will increase dramatically for the same amount of optical surface roughness[7]. This places strict requirements on the optical finish quality.

The amount of flare at a given point in the field is also dependent on lens traffic which is set by the local pattern density surrounding that point (points with more absorbing layer surrounding them have lower flare and vice versa) and the proximity to the field edge[1,5]. Therefore, the flare may vary significantly across the field, and this variation can lead to unwanted critical dimension variation. Therefore, some form of mask compensation may be required, possibly in the form of field-dependent CD resizing[8] or the use of dummy patterns to make the pattern density more uniform[5].

---

[1] Further author information: (Send correspondence to J.P.C., now with Advanced Micro Devices)
J.P.C.: E-mail: jason.cain@amd.com, Telephone: 1 (408) 749-2609

Several techniques have been developed for measuring and predicting flare in normal-incidence multilayer optics at EUV wavelengths, including angular scattering measurements[9,10], knife-edge measurements[11], predictions from surface roughness measurements[10-12], interferometric methods[13,14], and resist-based lithographic methods[4,15].

In order to investigate issues related to EUV lithography, a static micro-field exposure tool based on a 0.3-numerical aperture (NA) Micro-Exposure Tool (MET) optic and operating at a wavelength of 13.5 nm has been installed at the Advanced Light Source, a synchrotron facility at the Lawrence Berkeley National Laboratory[16-18]. The MET optic is composed of two multilayer-coated reflective elements and has a NA of 0.3, comparable to the value expected for first-generation EUV production tools, and a field size of 600 μm × 200 μm at the wafer. The flare in this optic was measured using a lithographic method described in Section 2. Measurement analysis in a scanning electron microscope (SEM) and in an optical microscope is discussed in Sections 3 and 4, respectively. The measurements are then compared with flare levels predicted from surface roughness measurements in Section 5, and conclusions are presented in Section 6.

2. MEASUREMENT TECHNIQUE

The flare in the MET optic was measured using a lithographic technique derived from Kirk's method[19]. This method has been used previously to characterize other EUV optics[4], and uses simple cross patterns of varying size placed in an otherwise bright field. The full field layout for the flare experiment is shown in Figure 1 while a closer view of the cross patterns is shown in Figure 2. Wafers were coated with a 125 nm thick layer of Rohm and Haas EUV-2D photoresist, and both post-application bake (PAB) and post-exposure bake (PEB) were performed at 130 °C. The wafers were then exposed using the mask pattern shown in Figure 1 and annular illumination with $\sigma_{inner} = 0.3$, $\sigma_{outer} = 0.7$, and $\lambda = 13.5$ nm. Flare for a given feature size is then defined as the exposure dose required to clear the resist in the bright region (E_0) divided by the dose to clear in the dark regions (E_{dark}):

$$\%\ \text{Flare} = \frac{E_0}{E_{dark}} \times 100 \ . \tag{1}$$

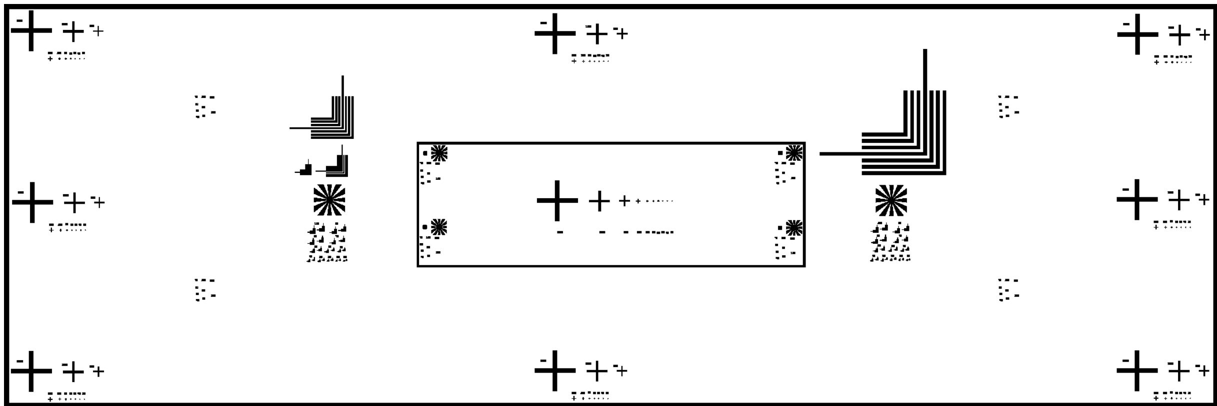

Figure 1. Field layout used for flare measurement. Field dimensions are 600 μm × 200 μm at the wafer.

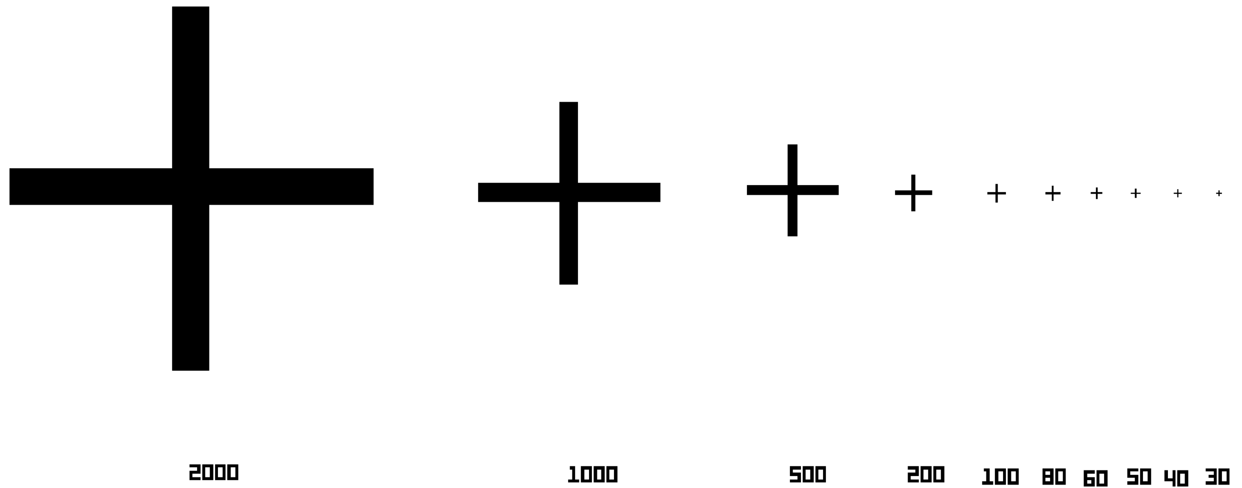

Figure 2. Cross patterns used for flare measurement. Numbers indicate cross arm width in nm.

3. MEASUREMENT RESULTS USING SCANNING ELECTRON MICROSCOPE

Flare measurements were initially performed using a scanning electron microscope (SEM). However, this led to unexpected results. As the exposure dose level was increased in an attempt to clear the resist in the cross patterns, the resist began to cross-link before the cross patterns disappeared. In a positive resist, cross-linking occurs when the exposed areas receive a very high dose that causes the resist molecules to link together. This cross-linking decreases the solubility of the resist relative to the unexposed areas, leading to a reversal of tone (*i.e.*, a positive resist will behave like a negative resist when cross-linking occurs). This is illustrated in Figure 3, showing the resist image of the cross patterns at a dose just below the cross-linking threshold, and Figure 4, showing the resist image at a dose just above the cross-linking threshold.

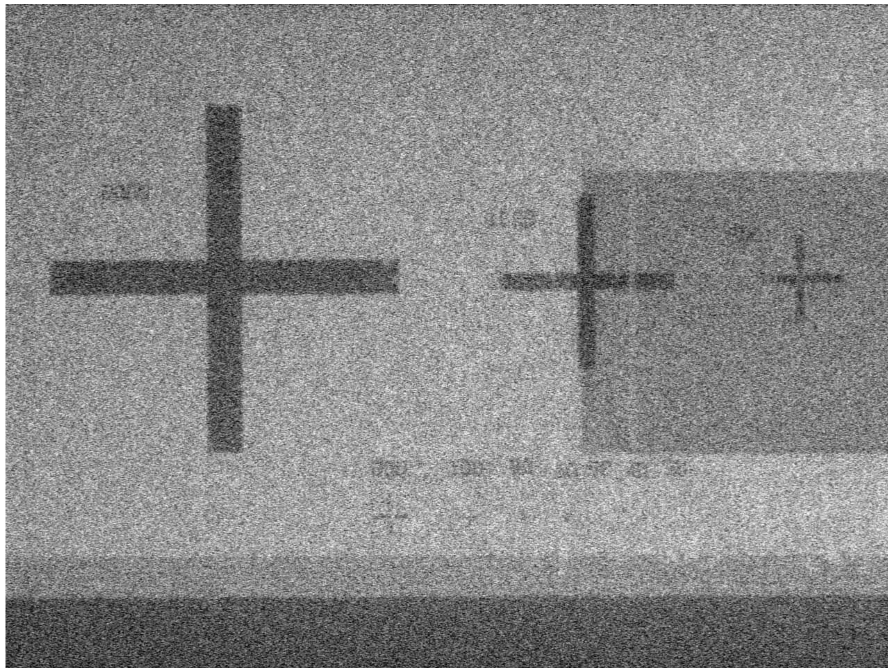

Figure 3. SEM image of cross patterns in Rohm and Haas EUV-2D resist at an exposure dose just below the cross-linking dose.

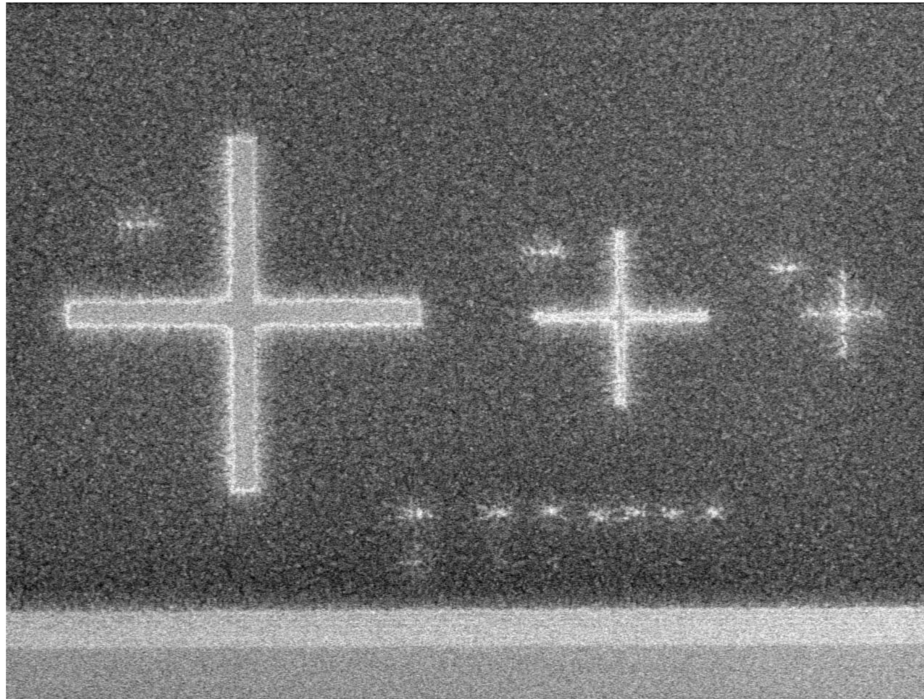

Figure 4. SEM image of cross patterns in Rohm and Haas EUV-2D resist at an exposure dose just above the cross-linking dose.

These observations from the SEM initially led to the conclusion that the dynamic range of the resist used (EUV-2D) was insufficient to measure the flare in the MET optic, and that the maximum measurable level of flare was less than 2%. However, this did not agree with the predicted intrinsic flare value of approximately 6.5% made from atomic-force microscopy (AFM) and optical scattering measurements of the surface roughness in the optic (discussed in Section 5). Subsequently, AFM measurements of the wafer surface at a dose just below the onset of cross-linking (as shown in Figure 3) showed that only a very thin (1-2 nm) layer of resist "scumming" remained on the wafer in the unexposed areas. Because of the difficulty in distinguishing resist patterns with full resist thickness, to patterns with only "scumming" in the SEM, it was determined that SEM analysis is an unreliable method for making flare measurements in resist, at least for the particular resist process used in this experiment.

4. MEASUREMENT RESULTS USING OPTICAL MICROSCOPE

The flare measurements were then repeated using an optical microscope (100× objective with differential interference contrast). This analysis yielded very different results, as the cross patterns disappeared in the optical microscope well before the onset of resist cross-linking (the "scumming" seen in the SEM was invisible in the optical microscope). Therefore, the optical microscope may serve as a more reliable analysis tool for measuring flare.

Across-field contour maps of the flare measurements made using the optical microscopes are shown for 500 nm, 1 μm, and 2 μm features in Figure 5, Figure 6, and Figure 7, respectively. Only the left side of the field is shown, as across-field illumination non-uniformity made interpretation of the results impossible at the right edge of the field.

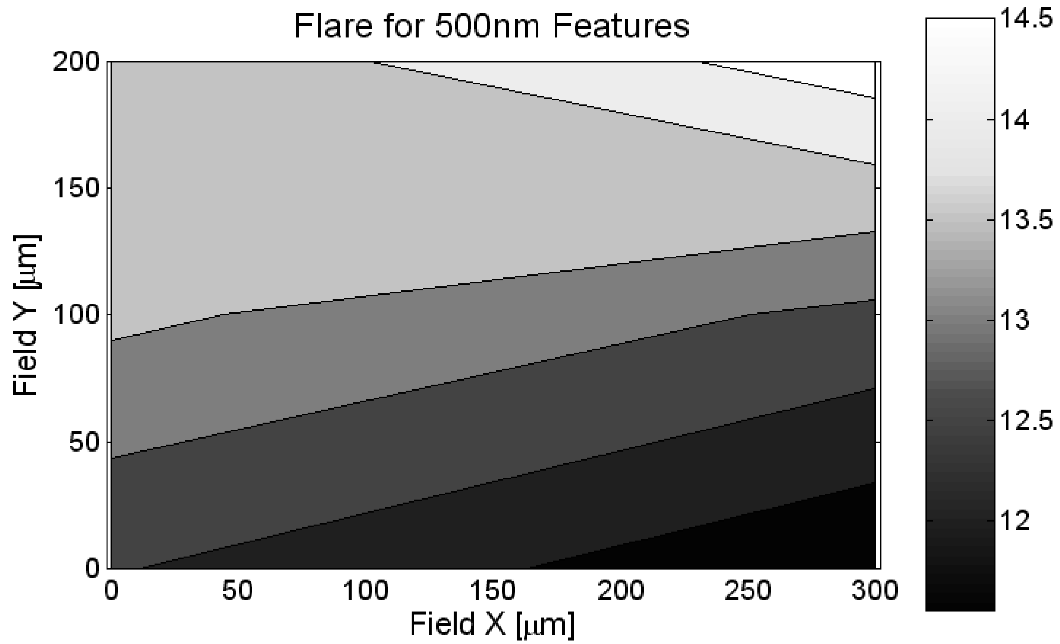

Figure 5. Flare for 500 nm features measured using an optical microscope. Only the left half of the field is shown, as across-field illumination non-uniformity prevented accurate measurements on the right side of the field.

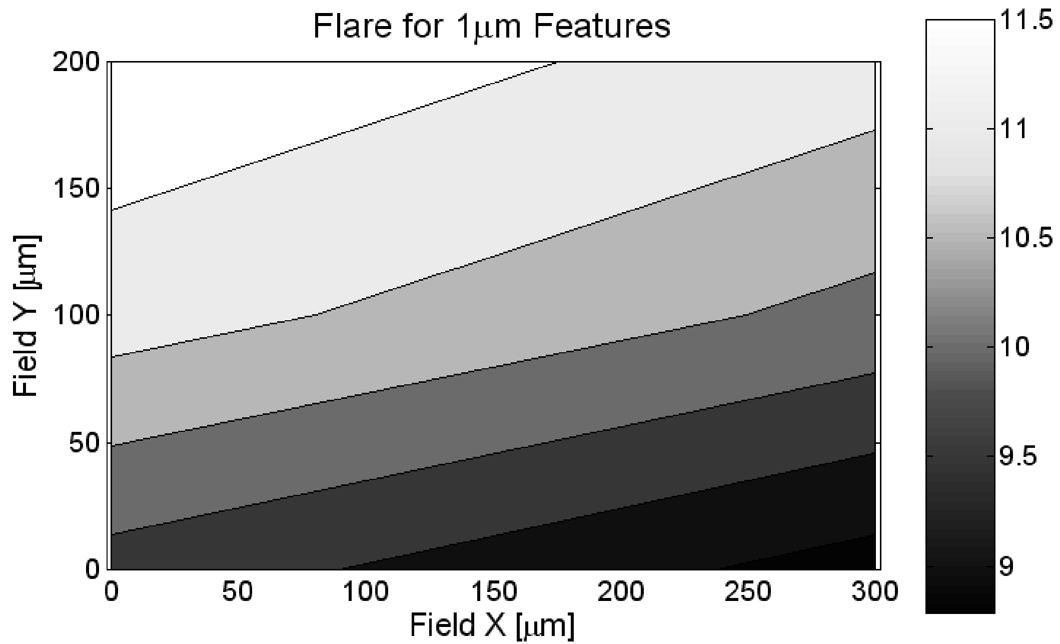

Figure 6. Flare for 1 μm features measured using an optical microscope. Only the left half of the field is shown, as across-field illumination non-uniformity prevented accurate measurements on the right side of the field.

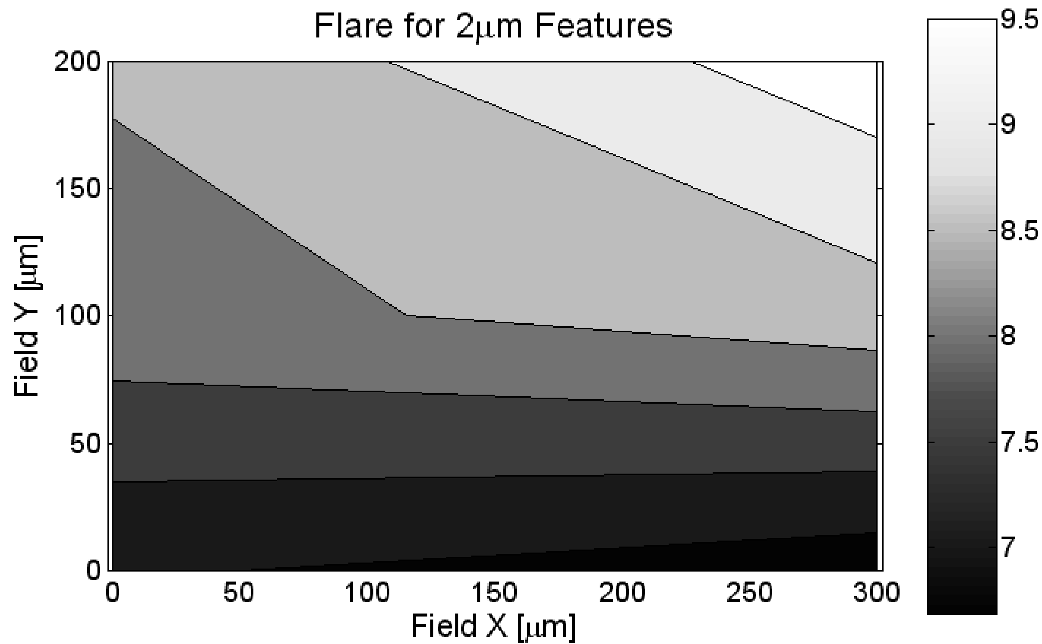

Figure 7. Flare for 2 μm features measured using an optical microscope. Only the left half of the field is shown, as across-field illumination non-uniformity prevented accurate measurements on the right side of the field.

5. COMPARISON WITH PREDICTED FLARE LEVELS

In order to validate the lithographic flare measurements, comparisons were made between the measured values and predicted levels based on power spectral density (PSD) of the surface roughness in the optic,[20] shown in Figure 8. The PSD data was used to predict the flare in an isolated line within a 600 μm × 200 μm field. The results of this prediction are shown along with the optical microscope measurements in Figure 9. The measured values of flare are higher than the predictions by a factor of approximately two.

Part of the apparent flare may be attributed to the non-ideal mask contrast (*i.e.*, the absorber pattern has non-zero reflectance). In order to determine the contribution of this effect, the *in-situ* dose sensor was used to measure the dose at the wafer plane with the illumination on both a large absorber area and a large multilayer reflective coated area. The ratio of the two dose measurements was 1%. Therefore, the cross patterns used in the flare experiments will receive an extra 1% background dose just from reflectance from the absorber pattern. This additional dose must be subtracted from the flare measurements in order to separate the contributions of flare and absorber reflectance. In addition, aerial image proximity effects contribute to the apparent flare seen at the wafer in the form of reduced contrast. These effects were simulated using aerial image modeling software along with lateral shearing interferometry measurements of the MET wavefront[21] and found to be 2% or less for the feature sizes measured here. The measured data was corrected for imperfect mask contrast and aerial image proximity effects, and the results are shown in Figure 10.

Although the corrected measurements are closer to the predicted values than the raw measurements, there is still a significant difference between the two. It was then theorized that this difference could be the result of relatively "long range" flare from surrounding fields in the focus-exposure matrix (FEM) on the wafer. The flare from surrounding fields will have an additive effect upon the measured flare due to the dose integrating behavior of photoresist.

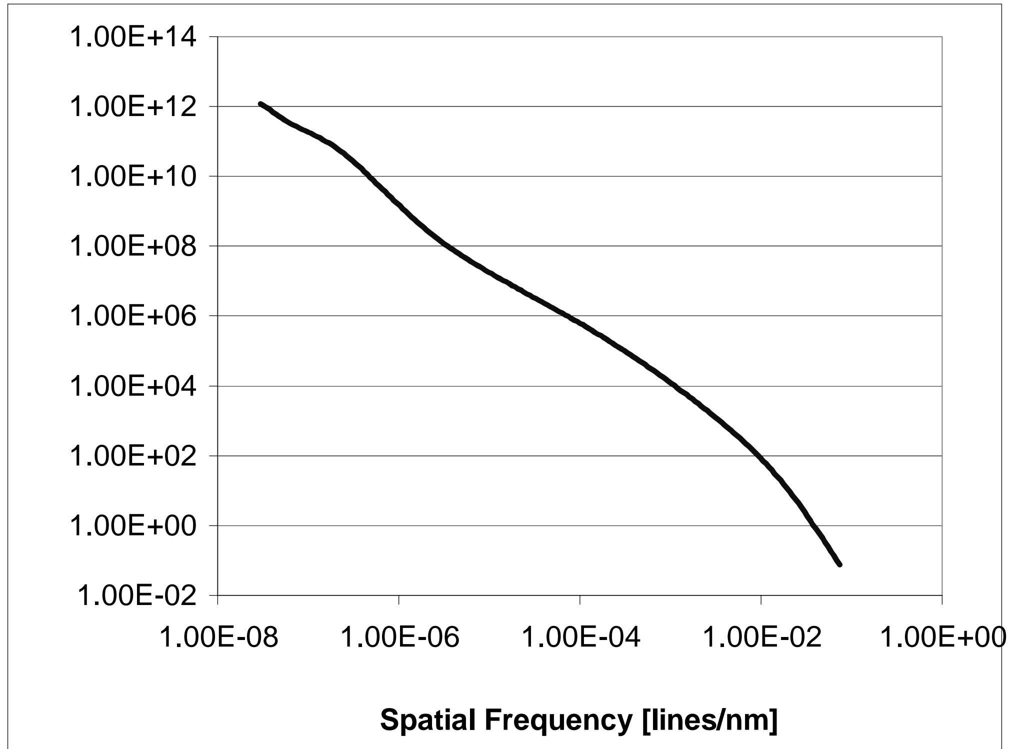

Figure 8. Power spectral density (PSD) of surface roughness in the MET optic. From E. Gullikson, LBNL[20].

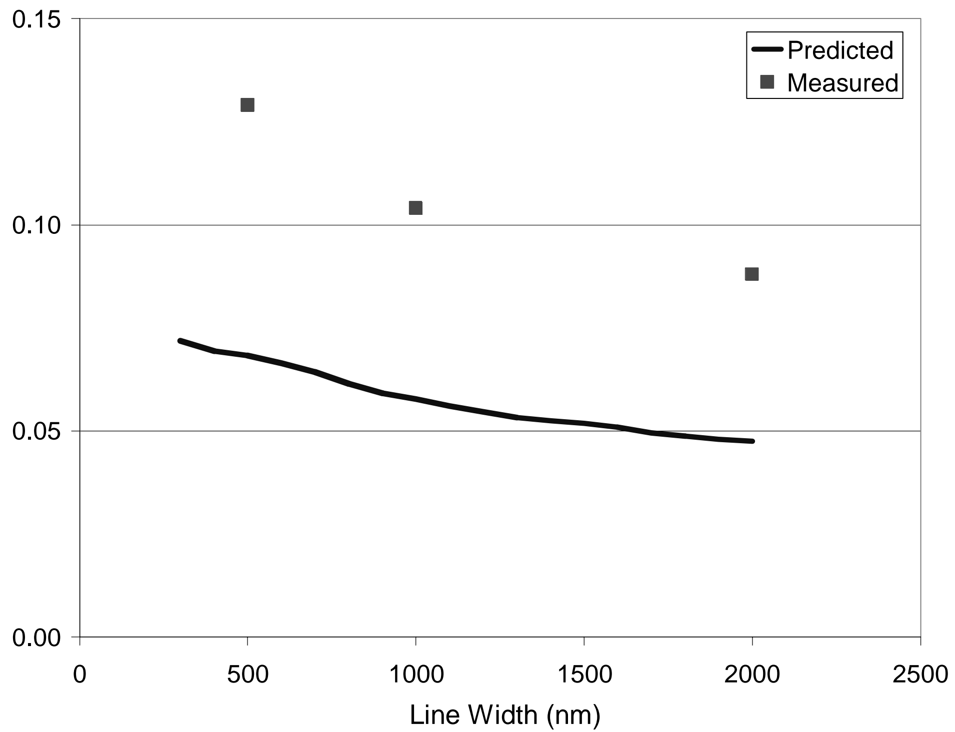

Figure 9. Comparison of flare in the MET optic as predicted from PSD data and measured with optical microscope.

A second experiment was performed to determine if the density of exposures within the FEM did in fact affect the measured flare. The resist type, thickness, and processing parameters were all identical to the first flare experiment. However, in this case, the spacing of exposures within the FEM was changed from 100 μm in both the *x*- and *y*-directions to 800 μm in the *x*-direction and 400 μm in the *y*-direction. The limited area accessible on the wafer (due to stage movement range limitations) and the need to print at a few different focus steps in order to ensure good focus made it necessary to restrict the range of dose values in order to fit the exposures into the allowable area of the wafer. The result of this restricted dose range was to limit the flare measurement to a single point within the field (variation in the relevant dose levels due to across-field illumination intensity non-uniformity caused the other points in the field to fall outside the restricted range). The center point of the field was chosen, and the dose targeted accordingly. The resulting flare measurements (made with an optical microscope) were then corrected for imperfect mask contrast and aerial image proximity effects. These results are shown in Figure 11 and marked as "Isolated Field". These flare measurements agree very well with predicted values.

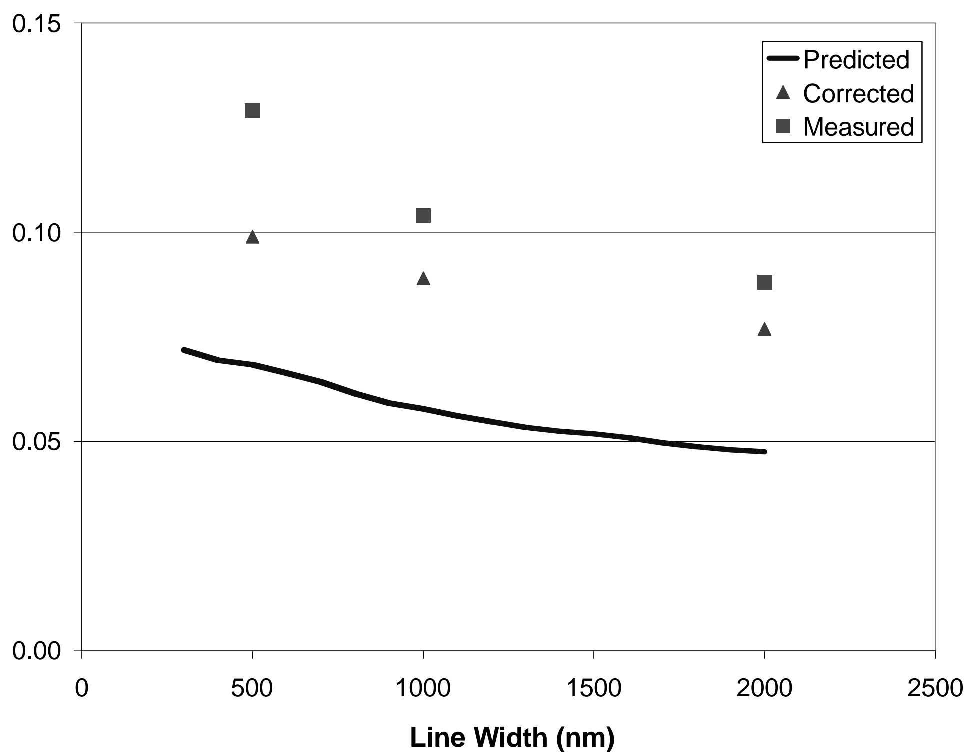

Figure 10. Comparison of predicted flare (from PSD) with raw measurements (from optical microscope) and measurements corrected for imperfect mask contrast and aerial image proximity effects.

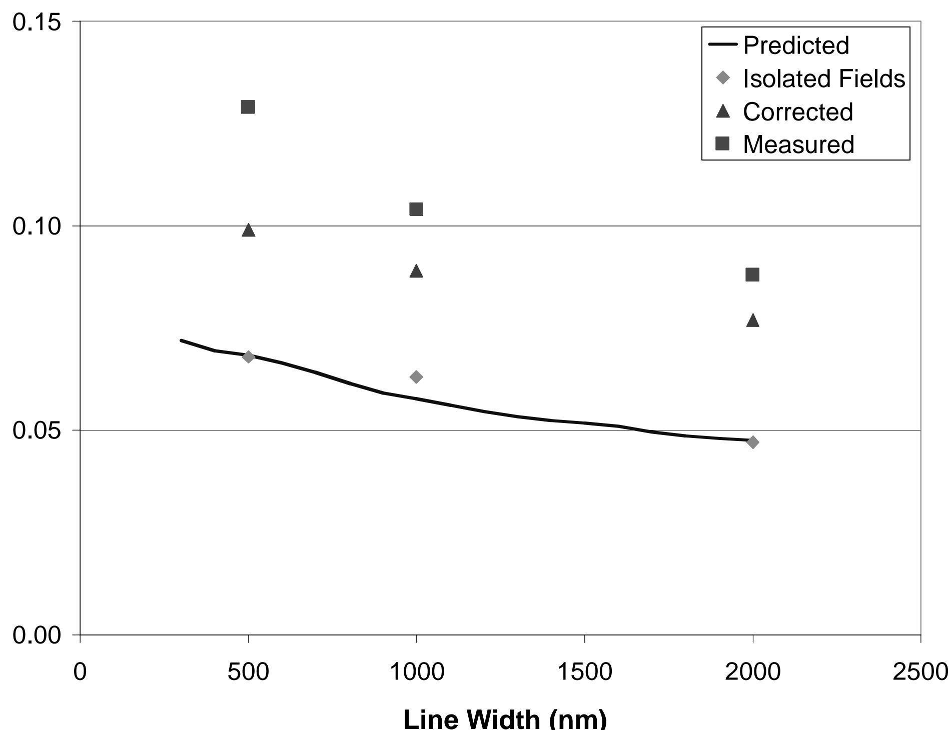

Figure 11. Comparison of predicted flare (from PSD) with raw measurements from optical microscope, measurements corrected for imperfect mask contrast and aerial image proximity effects, and "isolated" field measurements (also measured with optical microscope and corrected for imperfect mask contrast and aerial image proximity effects).

6. CONCLUSIONS

The amount of EUV flare was measured for the 0.3-NA MET optic at Lawrence Berkeley National Laboratory using a well-known technique (Kirk's method). Analysis was attempted using both a scanning electron microscope and an optical microscope, and the optical microscope was judged to be more reliable due to photoresist "scumming" behavior at high exposure doses which make it difficult to evaluate when the resist pattern is effectively cleared in the SEM. Measurements were then compared with predicted flare levels based on measurements of the surface roughness present in the optic. The raw measured data was found to be significantly higher than the predicted values (by roughly a factor of two). However, when the experiment was repeated with widely spaced fields in the exposure matrix and the data corrected for imperfect mask contrast and aerial image proximity effects, the measured results match the prediction very well. The amount of flare present in this optic ranges from ~5% for 2 μm features to ~7% for 500 nm features. Accurate measurement of the flare present in the MET system provides a benchmark for current EUV optics, and will also facilitate future research into methods for minimizing the effects of flare on desired circuit patterns.

ACKNOWLEDGMENTS

Many thanks are due to the excellent scientific and technical staff at CXRO, including Ken Goldberg, Paul Denham, Brian Hoef, and Erik Anderson. Thanks are also due to Kim Dean of SEMATECH for her support of this research, and to Robert Brainard of Rohm and Haas for resist support. Lawrence Berkeley National Laboratory is operated under the auspices of the Director, Office of Science, Office of Basic Energy Science, of the US Department of Energy. This work was funded by Advanced Micro Devices, Applied Materials, Atmel, Cadence, Canon, Cymer, DuPont, Ebara, Intel, KLA-Tencor, Mentor Graphics, Nikon Research, Novellus Systems, Panoramic Technologies, Photronics, Synopsis, Tokyo Electron, and the UC Discovery Grant.

REFERENCES

1. C. Krautschik, M. Ito, I. Nishiyama, and S. Okazaki, "Impact of EUV light scatter on CD control as a result of mask density changes," in *Emerging Lithographic Technologies VI*, R. L. Engelstad, ed., Proc. SPIE **4688**, pp. 289-310, 2002.
2. A. Bourov, L. C. Litt, and L. Zavyalova, "Impact of flare on CD variation for 248nm and 193nm lithography systems," in *Optical Microlithography XIV*, C. J. Progler, ed., Proc. SPIE **4346**, pp. 1388–1393, 2001.
3. L. C. Litt, A. Bourov, B. LaFontaine, and E. Apelgren, "Evaluation and characterization of flare in ArF lithography," in *Optical Microlithography XV*, A. Yen, ed., Proc. SPIE **4691**, pp. 1442–1452, 2002.
4. S. H. Lee, P. Naulleau, C. Krautschik, M. Chandhok, H. N. Chapman, D. J. O'Connell, and M. Goldstein, "Lithographic flare measurements of EUV full-field projection optics," in *Emerging Lithographic Technologies VII*, R. L. Engelstad, ed., Proc. SPIE **5037**, pp. 103–111, 2003.
5. M. Chandhok, S. H. Lee, C. Krautschik, B. J. Rice, E. Panning, M. Goldstein, and M. Shell, "Determination of the flare specification and methods to meet the CD control requirements for the 32 nm node using EUVL," in *Emerging Lithographic Technologies VIII*, R. S. Mackay, ed., Proc. SPIE **5374**, pp. 86–95, 2004.
6. J. C. Stover, *Optical Scattering Measurement and Analysis*, SPIE Optical Engineering Press, Bellingham, WA, Second Ed., 1995.
7. K. Lai, C.H. J. Wu, and C. J. Progler, "Scattered light: The increasing problem for 193nm exposure tools and beyond," in *Optical Microlithography XIV*, C. J. Progler, ed., Proc. SPIE **4346**, pp. 1424-1435, 2001.
8. C. Krautschik, M. Chandhok, G. Zhang, S. Lee, M. Goldstein, E. Panning, R. Bristol, and V. Singh, "Implementing flare compensation for EUV masks through localized mask CD resizing," in *Emerging Lithographic Technologies VII*, R. L. Engelstad, ed., Proc. SPIE **5037**, pp. 58–68, 2003.
9. E. Spiller, D. Stearns, and M. Krumrey, "Multilayer X-ray mirrors: Interfacial roughness, scattering, and image quality," *J. Appl. Phys.* **74**, pp. 107–118, 1 July 1993.
10. D. G. Stearns, D. P. Gaines, D. W. Sweeney, and E. M. Gullikson, "Nonspecular X-ray scattering in a multilayer-coated imaging system," *J. Appl. Phys.* **84**, pp. 1003–1028, 15 July 1998.
11. E. M. Gullikson, S. Baker, J. E. Bjorkholm, J. Bokor, K. A. Goldberg, J. E. M. Goldsmith, C. Montcalm, P. Naulleau, E. Spiller, D. G. Stearns, J. S. Taylor, and J. H. Underwood, "EUV scattering and flare of 10x projection cameras," in *Emerging Lithographic Technologies III*, Y. Vladimirsky, ed., Proc. SPIE **3676**, pp. 717–723, 1999.
12. E. M. Gullikson, "Scattering from normal incidence EUV optics," in *Emerging Lithographic Technologies II*, Y. Vladimirsky, ed., Proc. SPIE **3331**, pp. 72–80, 1998.
13. P. Naulleau, K. A. Goldberg, E. M. Gullikson, and J. Bokor, "Interferometric atwavelength flare characterization of extreme ultraviolet optical systems," *J. Vac. Sci. Technol. B* **17**, pp. 2987–2991, Nov./Dec. 1999.
14. P. Naulleau, K. A. Goldberg, E. M. Gullikson, and J. Bokor, "At-wavelength, system level flare characterization of extreme-ultraviolet optical systems," *Applied Optics* **39**, pp. 2941–2947, 10 June 2000.
15. P. Naulleau, K. A. Goldberg, E. Anderson, K. Bradley, R. Delano, P. Denham, B. Gunion, B. Harteneck, B. Hoef, H. Huang, K. Jackson, G. Jones, D. Kemp, J. A. Liddle, R. Oort, A. Rawlins, S. Rekawa, F. Salmassi, R. Tackaberry, C. Chung, L. Hale, D. Phillion, G. Sommargren, J. Taylor, "Status of EUV microexposure capabilities at the ALS using the 0.3-NA MET optic," in *Emerging Lithographic Technologies VIII*, R. Scott Mackay, ed., Proc. SPIE **5374**, pp. 881–891, 2004.
16. M. Chandhok, S. H. Lee, C. Krautschik, G. Zhang, B. J. Rice, M. Goldstein, E. Panning, R. Bristol, A. Stivers, and M. Shell, "Comparison of techniques to measure the point spread function due to scatter and flare in EUV lithography systems," in *Emerging Lithographic Technologies VIII*, R. S. Mackay, ed., Proc. SPIE **5374**, pp. 854–860, 2004.
17. P. Naulleau, K. A. Goldberg, E. Anderson, J. P. Cain, P. Denham, K. Jackson, A.-S. Morlens, S. Rekawa, F. Salmassi, "Extreme ultraviolet microexposures at the Advanced Light Source using the 0.3 numerical aperture micro-exposure tool optic," *J. Vac. Sci. Tech. B*, **22**(6), pp. 2962–2965, Nov./Dec. 2004.
18. P. P. Naulleau, K. A. Goldberg, E. H. Anderson, J. P. Cain, P. Denham, B. Hoef, K. Jackson, A. Morlens, S. Rekawa, "EUV microexposures at the ALS using the 0.3-NA MET projection optics," in *Emerging Lithographic Technologies IX*, R. Scott Mackay, ed., Proc. SPIE **5751**, 2005.
19. J. P. Kirk, "Scattered light in photolithographic lenses," in *Optical/Laser Microlithography VII*, T. A. Brunner, ed., Proc. SPIE **2197**, pp. 566–572, 1994.
20. E. M. Gullikson, private communication, 2004.

21. K. A. Goldberg, P. Naulleau, P. Denham, S. B. Rekawa, K. Jackson, J. A. Liddle, E. H. Anderson, "EUV interferometric testing and alignment of the 0.3 NA MET optic," in *Emerging Lithographic Technologies VIII*, R. Scott Mackay, ed., Proc. SPIE **5374**, pp. 64–73, 2004.